ISSN 1070-3284, Russian Journal of Coordination Chemistry, 2017, Vol. 43, No. 9, pp. 604–611. © Pleiades Publishing, Ltd., 2017.

A 3D Europium-Organic-Framework from Phenyl Imidazole Dicarboxylate Showing High Sensitivity in Detection of Nitrobenzene[1]

Q. Y. Huang[a], Y. Zhao[b], L. Fu[c], and G. Li[c, *]

[a] *Department of Chemical Engineering, Henan Polytechnic Institute, Nanyang Henan, 473009 P.R. China*

[b] *Department of Chemical Engineering, Henan Vocational College of Applied Technology, Zhengzhou Henan, 450042 P.R. China*

[c] *College of Chemistry and Molecular Engineering, Zhengzhou University, Zhengzhou Henan, 450001 P.R. China*

**e-mail: gangli@zzu.edu.cn*

Received October 16, 2016

Abstract—A Eu-based luminescent MOF, namely, $\{[Eu(\mu_3\text{-HPhIDC})(\mu_2\text{-}C_2O_4)_{0.5}(H_2O)] \cdot 2H_2O\}_n$ (**I**) (H_3PhIDC = 2-phenyl-1*H*-imidazole-4,5-dicarboxylic acid) has been hydrothermally synthesized and structurally characterized by single-crystal X-ray diffraction techniques (CIF file CCDC no. 1457365). The MOF **I** indicates characteristic sharp emission bands of Eu^{3+} ion, which is selectively sensitive to nitrobenzene-based derivatives (nitrobenzene, 2-nitrotoluene, 3-nitrotoluene, 1,3-dinitrobenzene and 2,4-dinitrotoluene). These properties make **I** a potential fluorescence sensor for these chemicals.

Keywords: Eu(III) MOF, imidazole dicarboxylate, nitrobenzene, chemosensor

DOI: 10.1134/S1070328417090032

INTRODUCTION

Luminescence is one of the important properties of metal-organic frameworks (MOFs) [1–3]. However, the exploration of practical applications for luminescent MOFs remains in the early stage of development. Molecular recognition properties of the luminescent MOFs have attracted much attention [4–7]. Because when people embedded a photoactive molecule into a framework scaffold and fabricated a luminescent framework that distinguishes among molecules using multi-color emissions originated from the guest-framework interaction. This system also allows people to investigate fundamental photo-physical processes based on molecular interactions, since the porous framework gives serves as a solid-state matrix in which the individual molecules are spatially confined. In this context, although there are some MOFs showing sensitivity in detection of nitrobenzene (NB) [8–13], reports on imidazole dicarboxylate-based polymers having the recognition properties of NB are rare. Indeed, there is only one example of such polymers in reference [14], in which Y.L. Li and coauthors have reported that a novel terbium-organic-framework, $\{(Tb(\mu_3\text{-HPhIDC})(\mu_2\text{-}C_2O_4)_{0.5}(H_2O)) \cdot 2H_2O\}_n$ (H_3PhIDC = 2-phenyl-1*H*-imidazole-4,5-dicarboxylic acid) exhibits selective detection of nitrobenzene via a photoinduce electron transfer quenching mechanism [14]. This interesting finding prompted us to construct more similar MOFs as fluorescence sensors for NB.

Considering the types of Eu^{3+} MOFs usually showing characteristic, easily separable, line-like emission bands [15], and having long-lived excited state lifetimes in the ms-range, they usually have been used to explore their sensing properties. As a contribution to such chemistry, herein we still choose the promising bridging ligand, H_3PhIDC to react with Eu^{3+} ion under hydrothermal conditions, and get a 3D luminescent MOF, $\{[Eu(\mu_3\text{-HPhIDC})(\mu_2\text{-}C_2O_4)_{0.5}(H_2O)] \cdot 2H_2O\}_n$ (**I**), which is isostructural with the reported Tb-MOF, $\{(Tb(\mu_3\text{-HPhIDC})(\mu_2\text{-}C_2O_4)_{0.5}(H_2O)) \cdot 2H_2O\}_n$ (**II**) [14]. Further investigation shows that **I** has high sensitivity and quick response toward the presence of trace amount of nitrobenzene and the related derivatives.

EXPERIMENTAL

All chemicals were of reagent grade quality obtained from commercial sources and used without further purification. The organic ligand H_3PhIDC was prepared according to [16, 17].

The C, H and N analyses were carried out on a FLASH EA 1112 analyzer. IR spectra were recorded on a BRUKER TENSOR 27 spectrophotometer as KBr pellets in the 400–4000 cm^{-1} region. Thermogravimetric (TG) analysis measurements were per-

[1] The article is published in the original.

formed by heating the crystalline samples from 20 to 850°C at a rate of 10°C min^{-1} in air on a Netzsch STA 409PC differential thermal analyzer. X-ray powder diffraction (PXRD) measurements were recorded on a Panalytical X'pert PRO X-ray diffractometer. Fluorescence spectra were characterized at room temperature by a F-7000 fluorescence spectrophotometer.

Synthesis of I. A mixture of $Eu(NO_3)_3 \cdot 6H_2O$ (44.6 mg, 0.1 mmol), H_3PhIDC (25.0 mg, 0.1 mmol), H_2O (7 mL) and oxalic acid (12.6 mg, 0.1 mmol) was sealed in a 25 mL Teflon-lined bomb and heated at 160°C for 72 h, and then cooled to room temperature at a rate of 10°C/h. The light-yellow rhombus crystals of **I** were collected, washed with distilled water, and dried in air (68% yield based on Eu).

IR (KBr; ν, cm^{-1}): 3446 m, 3154 m, 2919 w, 1633 w, 1549 s, 1489 w, 1403 s, 1383 s, 1268 w, 1286 m, 1260 m, 1128 s, 1021 w, 823 s, 733 m, 561 m, 533 w, 517 w, 440 m.

For $C_{12}H_{12}N_2O_9E$			
Anal. calcd, %:	C, 52.62;	H, 3.56;	N, 9.03.
Found, %:	C, 52.44;	H, 3.78;	N, 9.41.

Luminescence measurements and experiment for the detection of nitro compounds were performed in a manner analogous as described in reference [14], only **I** was used instead of $\{(Tb(\mu_3\text{-}HPhIDC)(\mu_2\text{-}C_2O_4)_{0.5}(H_2O)) \cdot 2H_2O\}_n$.

X-ray structure determination. Suitable single crystal of compound **I** was selected for single-crystal X-ray diffraction analyses. The intensity data were measured on a Bruker Smart 1000 diffractometer with a graphite-monochromated MoK_α radiation (λ = 0.71073 Å). Single crystal of **I** was selected and mounted on a glass fiber. All data were collected at room temperature using the ω–2θ scan technique and corrected for Lorenz-polarization effects. A correction for secondary extinction was applied.

The structure was solved by direct methods and expanded using the Fourier technique. The non-hydrogen atoms were refined with anisotropic thermal parameters. All the hydrogen atoms were included in the final refinement. The final cycle of full-matrix least squares refinement was based on 2589 observed reflections and 238 variable parameters for **I**. All calculations were performed using the SHELX-97 crystallographic software package [18]. The crystallographic data and selected bond lengths and angles are given in Tables 1 and 2, respectively. Supplementary material for structure **I** has been deposited with the Cambridge Crystallographic Data Centre (CCDC no. 1457365; deposit@ccdc.cam.ac.uk or http://www.ccdc.cam.ac.uk).

RESULTS AND DISCUSSION

Single-crystal X-ray diffraction analysis shows that **I** is a (3,4)-connected 3D network. As shown in Fig. 1a the asymmetric unit of **I** consists of three $HPhIDC^{2-}$ ligands, one bidentate chelating co-ligand $\mu_2\text{-}C_2O_4^{2-}$, one coordinated and two free water molecules, and one Eu^{3+} ion. Each Eu^{3+} ion is eight-coordinated by four oxygen and one nitrogen atoms from three individual $HPhIDC^{2-}$ anions, two oxygen atoms from the oxalate ligand and one coordinated water molecule forming a distorted bicapped trigonal prism coordination polyhedron (Fig. 1a). The Eu–O/N bond lengths are in the range of 2.307(3)–2.617(3) Å. The bond angles around each Eu^{3+} ion vary from 66.79(10)° to 151.21(10)°, which are consistent with the reported values in other Eu-containing complexes with similar organic ligands [19, 20]. Each $HPhIDC^{2-}$ anion adopts a μ_3-*k*N,O: *k*O',O'':*k*O''' mode to bridge neighboring Eu^{3+} ions (Fig. 1b). The Eu^{3+} ions form a dinuclear secondary building unit (SBU) via the chelating and bridging $HPhIDC^{2-}$ ligand with a metal separation of 6.7 Å, resulting in helical chains with a Eu(III)···Eu(III) separation of 5.7 Å through the $HPhIDC^{2-}$ ligand. As an auxiliary ligand, the oxalate ion coordinated with reverse bidentate mode μ_2-*k*O,O:*k*O,O. As viewed from Fig. 2a, neighboring Eu atoms are linked by $HPhIDC^{2-}$ to form a 1D helical chain along the *x* axis, and are further bridged by $\mu_2\text{-}C_2O_4^{-}$ ligands to generate a diamond-shaped 2D layer (Fig. 2b). Moreover, oxalates extended the two-dimensional sheets into a three-dimensional solid-state structure (Fig. 1c). Because MOF **I** is isostructural with the reported Tb-MOF II [14], **I** can also be considered as a (3,4)-connected network with the point symbol of $(4.8^5)(4.8^2)$.

The IR spectrum of **I** displays characteristic absorption bands for water molecules, carboxylate, imidazolyl, phenyl units and methyl substituent on the benzene ring. The strong and broad absorption bands in the range 3400–3500 cm^{-1} indicate the presence of the ν(N–H) and the ν(O–H) stretching frequencies of the imidazole ring and coordinated water molecules. The strong absorption bands around 1670 cm^{-1} are assigned to $\nu_{as}(COO^-)$ vibrations for the carboxyl groups. The characteristic bands at 736–879 cm^{-1} imply bending vibration (δ =C–H) bands of the phenyl ring.

Through TG analysis of **I** within the range of 20 to 850°C in air, we acquire the thermal stabilities for further exploration (Fig. 3). The TG of **I** indicates that the first weight loss of 19.85% occurs in the region of 30–245°C corresponding to the release of the free and coordinated waters (obsd. 4.84%, calcd. 5.06%). Secondly, it keeps losing weight from 245 to 712.5°C corresponding to the collapse of $HPhIDC^{2-}$ and $C_2O_4^{2-}$ units (obsd. 53.67%, calcd. 52.06%). Finally, a plateau

Table 1. Crystallographic data and structure refinement details for compound **I**

Parameter	Value
Fw	480.20
Crystal system	Monoclinic
Space group	$P2_1/c$
Crystal size	0.23 × 0.22 × 0.20
a, Å	9.1641(11)
b, Å	13.8913(17)
c, Å	11.6898(14)
β, deg	91.055(2)
V, Å^3	1487.9(3)
Z	4
ρ_{calcd}, mg m^{-3}	2.144
F(000)	932
μ, mm^{-1}	4.268
Reflectionns collected/unique (R_{int})	6126/2589 (0.0325)
Data/restraints/parameters	2589/10/238
Goodness-of-fit on F^2	1.007
Final *R* indices ($I > 2\sigma(I)$)	$R_1 = 0.0244$, $wR_2 = 0.0544$
R indices (all data)	$R_1 = 0.0317$, $wR_2 = 0.0570$
Largest difference peak and hole, *e* Å^{-3}	1.768 and −1.652

region is observed from 712.5 to 800°C, indicating that the final product is $0.5Eu_2O_3$ (obsd. 41.49%, calcd. 42.88%). In one word, the IR and thermal data of **I** are in reasonable agreement with the crystal structure analysis.

Because the isostructural Tb-Based MOF (II) [14] has shown selective and efficient emission quenching response upon interaction with nitroaromatic compounds, this reminds us that **I** also may be a good sensor for NB and the related derivatives. Thus, the photoluminescent properties of **I** have been investigated in the solid state at room temperature. As indicated in reference [16], the free H_3PhIDC ligand displays luminescence, with the emission maximum at 473 and 345 nm, respectively, which is attributed to the $\pi^* \rightarrow n$ transition. Compared with the H_3PhIDC ligand, **I** shows very different photoluminescent properties exhibiting strong red luminescence and characteristic transition spectrum of Eu^{3+} ion under excitation at 250 nm. It displays peaks at 593 nm and 616 nm corresponding to $^5D_0$–$^7F_1$ and $^5D_0$–$^7F_2$, transitions of Eu^{3+} ion, respectively. Usually, the emission band $^5D_0$–$^7F_2$ is distinctly stronger than the other emission bands $^5D_0$–^7F_J ($J = 0, 1, 2, 3, 4$) [20].

Table 2. Selected bond distances (Å) and angles (deg) for **I***

Bond	*d*, Å	Bond	*d*, Å
Eu(1)–O(2)	2.307(3)	Eu(1)–O(3)	2.321(3)
Eu(1)–O(1)$^{\#2}$	2.393(3)	Eu(1)–O(6)	2.395(3)
Eu(1)–O(5)$^{\#3}$	2.474(3)	Eu(1)–N(1)$^{\#2}$	2.617(3)
Eu(1)–O(4)$^{\#1}$	2.385(3)	Eu(1)–O(7)	2.474(3)
Angle	ω, deg	Angle	ω, deg
O(2)Eu(1)O(4)$^{\#1}$	139.86(11)	O(3)Eu(1)O(4)$^{\#1}$	78.86(10)
O(3)Eu(1)O(1)$^{\#2}$	151.21(10)	O(2)Eu(1)O(6)	141.17(10)
O(4)$^{\#1}$Eu(1)O(6)	75.56(10)	O(1)$^{\#2}$Eu(1)O(6)	75.68(10)
O(3)Eu(1)O(7)	137.00(11)	O(4)$^{\#1}$Eu(1)O(7)	141.69(11)
O(6)Eu(1)O(7)	81.02(12)	O(2)Eu(1)O(5)$^{\#3}$	76.92(10)
O(6)Eu(1)O(5)$^{\#3}$	66.79(10)	O(7)Eu(1)O(5)$^{\#3}$	70.85(11)
O(3)Eu(1)N(1)$^{\#2}$	105.47(11)	O(6)Eu(1)N(1)$^{\#2}$	139.51(10)
O(5)$^{\#3}$Eu(1)N(1)$^{\#2}$	149.38(10)	O(2)Eu(1)O(3)	76.12(10)
O(2)Eu(1)O(7)	74.28(11)	O(2)Eu(1)O(1)$^{\#2}$	122.19(10)
O(1)$^{\#2}$Eu(1)O(7)	71.79(10)	O(3)Eu(1)O(6)	104.45(11)
O(3)Eu(1)O(5)$^{\#3}$	72.57(11)	O(2)Eu(1)N(1)$^{\#2}$	73.08(11)

* Symmetry transformations used to generate equivalent atoms for **I**: $^{\#1}$ $-x+1, -y+1, -z+2$; $^{\#2}$ $x, -y+3/2, z+1/2$; $^{\#3}$ $-x, -y+1, -z+2$.

To further explore potential applications of **I** for probing small molecules, we started with common organic reagents to test the luminescence properties of **I**. In these experiments, the finely ground samples of **I** (3 mg) was dispersed in 3 mL of different solvents, including water, acetone, THF, DMF (*N*,*N*-dimethylformamide), acetonitrile, alcohols (methanol, ethanol, and *n*-butyl alcohol), chloroalkanes (CH_2Cl_2, $CHCl_3$), aldehydes (methanal, glyoxal) and other aromatic complexes (benzene, methylbenzene, benzaldehyde), treated by ultrasonication for 30 min, and then formed stable suspensions for fluorescence studies. The significant luminescent intensity quenching was observed only for nitrobenzene. As shown in Fig. 4, it could be found that the types of solvent: water, acetone, $CHCl_3$, benzene and ethanol did not strongly affect the luminescence intensity of **I**. While other solvents DMF, THF, methanal, benzaldehyde, and glyoxal have different levels of quenching effects on the luminescent intensity. The results demonstrate that **I** has high selectivity for nitrobenzene compared to other solvent molecules. That is to say, nitrobenzene makes the fluorescence intensity of compound basically quenched.

To examine the sensing sensitivity towards nitrobenzene in detail, a batch of suspensions of compound **I** dispersed in acetone solution treated by ultrasonication to form a stable suspension and solution. Then the fluorescence sensing ability of **I** was examined with gradually increasing nitrobenzene contents were prepared, and their emission spectra were recorded (since **I** dispersed in acetone solvent shows same emission

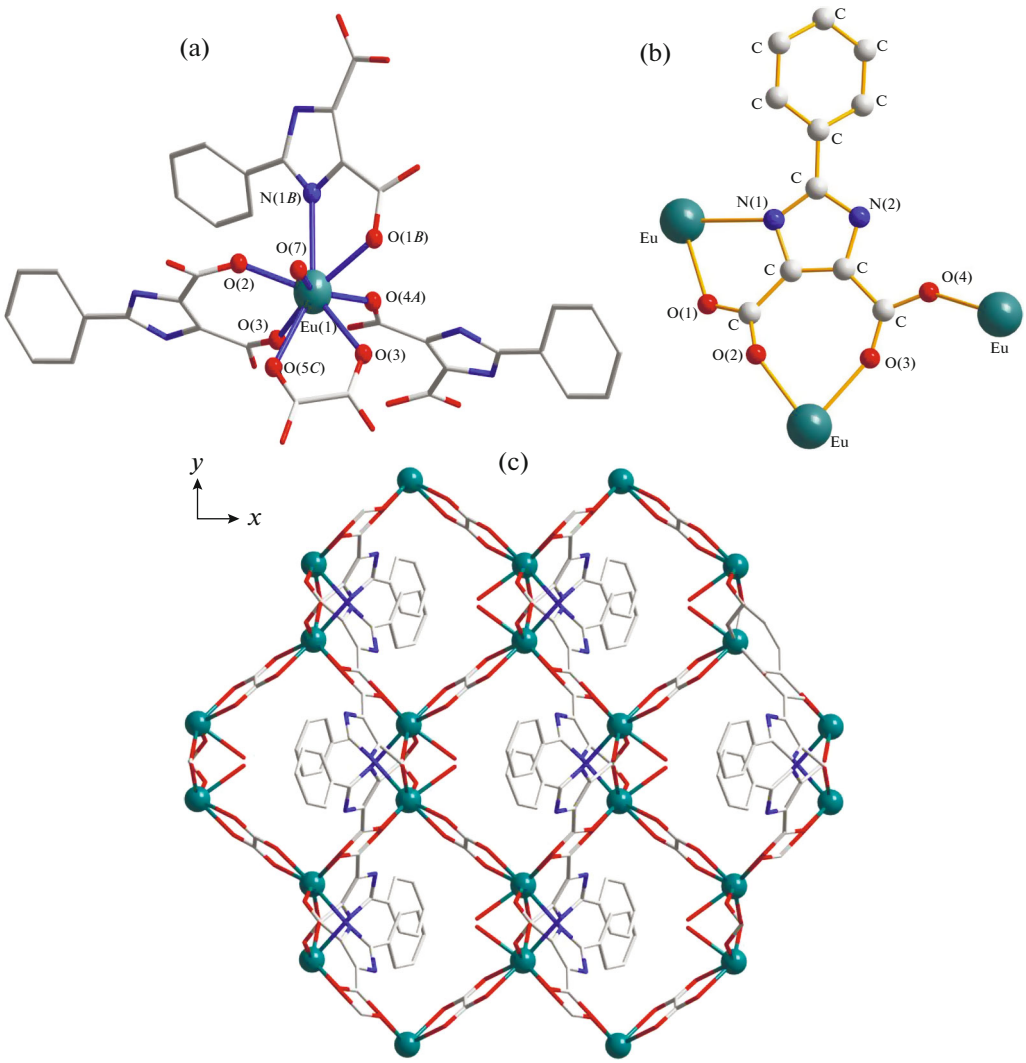

Fig. 1. Coordination environment of Eu^{3+} atom in **I** (H atoms omitted for clarity) (a); coordination mode of $HPhIDC^{2-}$ anion in **I** (b); schematic view of the 3D framework of **I** (c).

spectra as the solid-state sample, acetone was utilized as dispersion medium). As depicted in Fig. 5, it can be clearly seen that the fluorescence intensity gradually decrease with increase of nitrobenzene content, which indicates that **I** is a promising fluorescent probe for detecting nitrobenzene.

To investigate its sensitivity of the related compounds of nitrobenzene, we determined the fluorescent quenching properties of other nitroaromatic compounds, 2-nitrotoluene (2-NT), 3-nitrotoluene (3-NT), 1,3-dinitrobenzene (1,3-DNB) and 2,4-dinitrotoluene (2,4-DNT). The results show that the four nitroaromatic explosives also have a significant impact on quenching the fluorescence, among them 1,3-DNB quenches the luminescent intensity most conspicuous (2-NT 97.50%, 3-NT 96.15%, 1,3-DNB 96.35%, 2,4-DNT 97.13%, quenching percentage = $(I_0-I)/I_0 \times 100\%$, where I_0 and I are fluorescent intensities of **I** before and after exposure to the nitroaromatic explosive). That is to say, compound **I** also has extremely sensitive detection ability for other nitro-aromatic compounds (Fig. 6).

To explain the quenching mechanism of NB to **I**, we determined the PXRD spectra of the as synthesized products, which are in good agreement with the corresponding simulated ones. Furthermore, as described in reference [14], the PXRD data of **I** before or after immersing in different solvents have been performed, and show no difference. Thus we draw a conclusion that the crystal structure has not changed after treated with various solvents. Because the crystal structure, sensing properties, and PXRD data for NB of **I** are similar as the reported MOF II, so we approve the

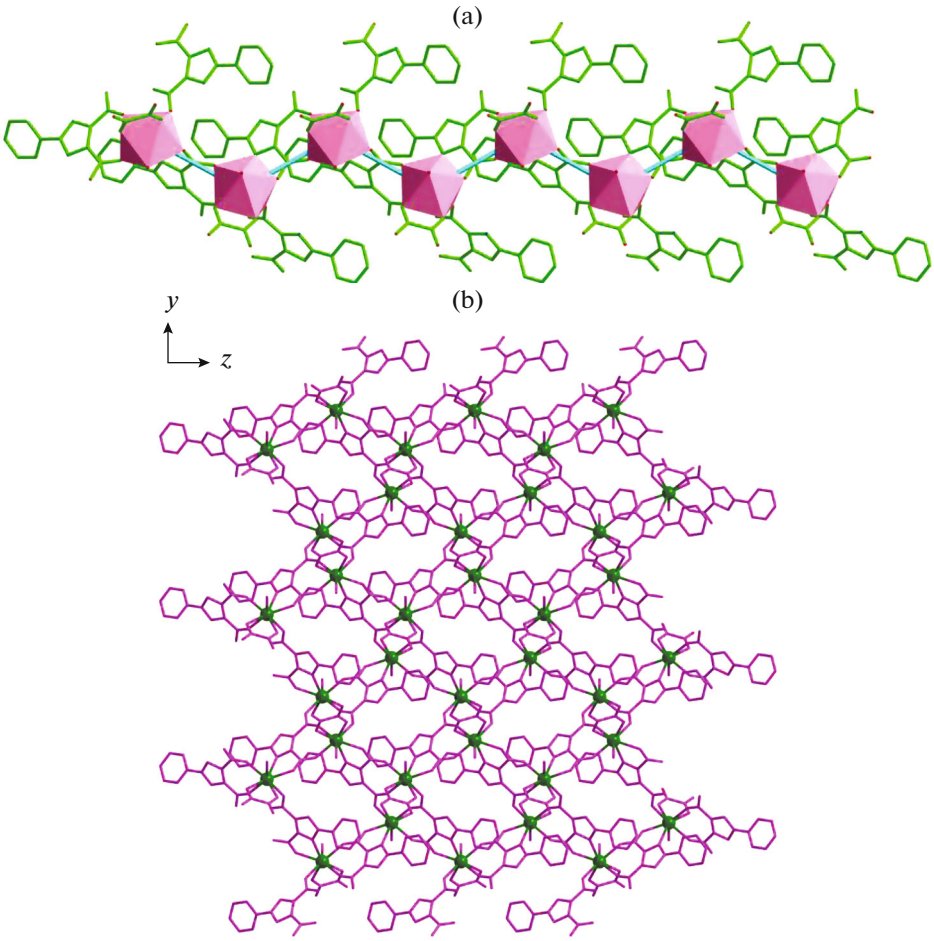

Fig. 2. Neighboring Eu atoms are linkedby $HPhIDC^{2-}$ to form 1D helical chain along the *x* axis (a); 1D helical chain bridged by μ_2-$C_2O_4^-$ ligands to generate a diamond-shaped 2D layer (b).

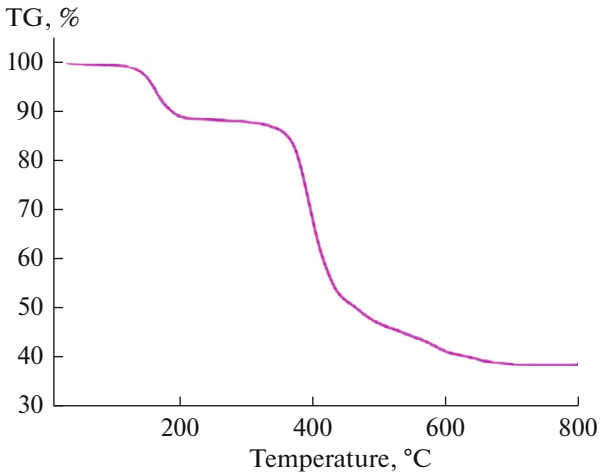

Fig. 3. The TG analysis profile of **I**.

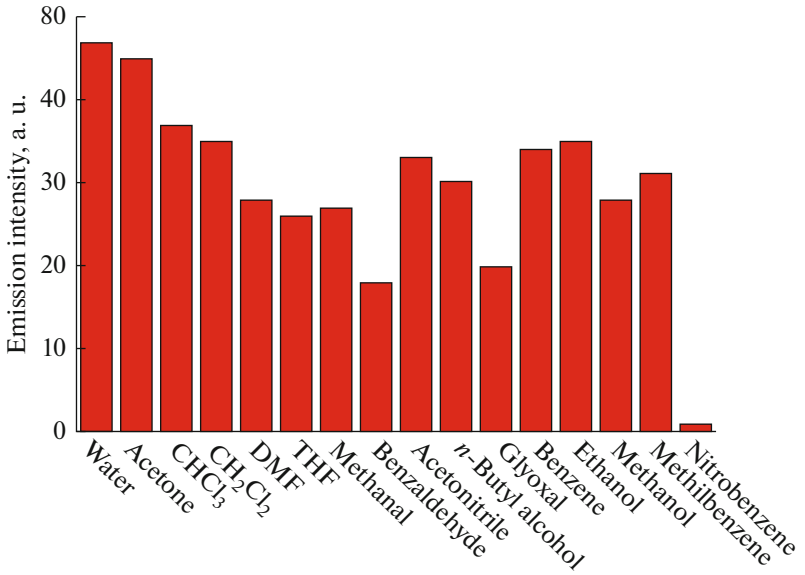

Fig. 4. Photoluminescence intensity of the $^5D_0 \rightarrow /^7F_2$ transition of **I** dispersed in different solvents, excited at 250 nm.

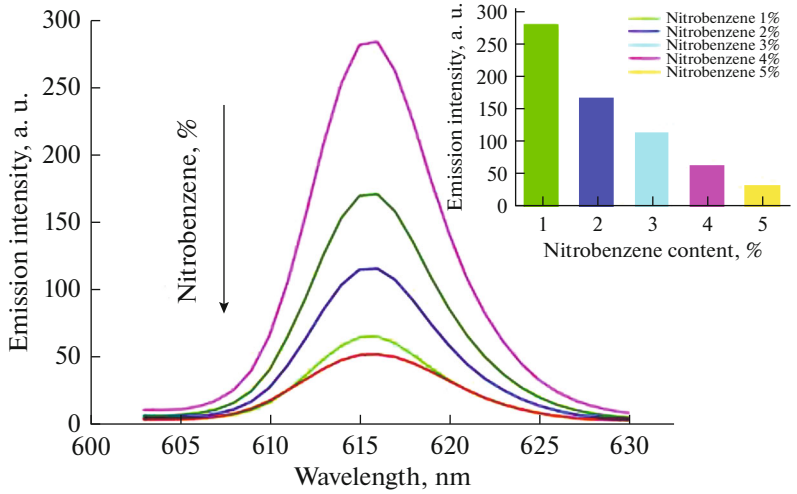

Fig. 5. Emissive response spectra of **I** for nitrobenzene in acetone solution with different nitrobenzene volume concentrations (insert is graph of the fluorescent intensity of **I,** acetone as a function of nitrobenzene content).

proposed quenching mechanism: the electron rich property of the H_3PhIDC ligand gives a higher LUMO energy than the tested nitroaromatics. Therefore, the excited state electrons transfer from the frameworks of the compounds to nitrobenzene, which leads to luminescence quenching [14].

The sensing ability of **I** could be regenerated and reused even after several cycles of sequential alternative addition of acetone and nitrobenzene and can be repeated for at least 5 times, indicating that **I** possesses high stability for its repeated usage in nitrobenzene detection (Fig. 7).

In summary, we have successfully synthesized a luminescent Eu-MOF via hydrothermal reactions. The MOF shows selective, sensitive, stable and efficient emission quenching response upon nitroaromatic compounds, all the results reveal that **I** is a promising candidate for detection of nitrobenzene and the related compounds.

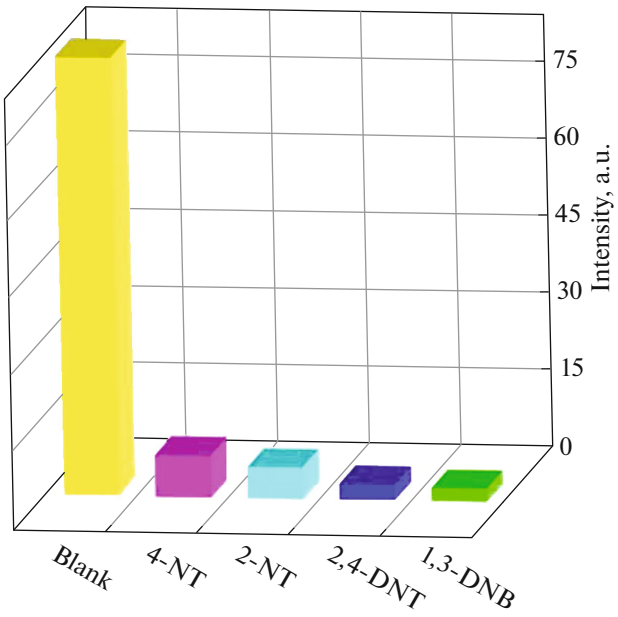

Fig. 6. Fluorescence quenching of **I** by different nitroaromatic compounds at room temperature.

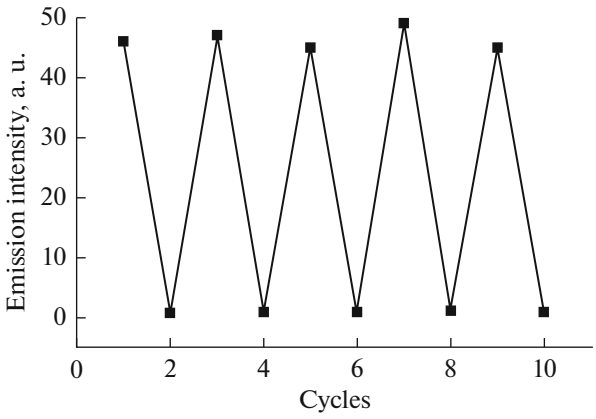

Fig. 7. The quenching and recovery test of **I** in acetone solution (the up dots represent the initial luminescent intensity and the down dots represent the intensity upon addition of nitrobenzene).

ACKNOWLEDGMENTS

The authors gratefully acknowledge the financial support by the National Natural ScienceFoundation of China (no. 21571156), (grant number J1210060), and Henan Province Foundation and Advanced Technology Research Project (no. 162300410206).

REFERENCES

1. Buenzli, J.-C.G., *J. Coord. Chem.*, 2014, vol. 67, p. 23.
2. Cui, Y., Yue, Y., Qian, G., et al., *Chem. Rev.*, 2012, vol. 112, p. 1126.
3. Allendorf, M.D., Bauer, C.A., Bhakta, R.K., et al., *Chem. Soc. Rev.*, 2009, vol. 38, p. 1330.
4. Cui, Y.J., Chen, B.L., and Qian, G.D., *Coord. Chem. Rev.*, 2014, vol. 273, p. 76.
5. Wang, C., Liu, D.M., and Lin, W.B., *J. Am. Chem. Soc.*, 2013, vol. 135, p. 13222.
6. Kreno, L.E., Leong, K., Farha, O.K., et al., *Chem. Rev.*, 2012, vol. 112, p. 1105.
7. Hu, Z.C., Deibert, B.J., and Li, J., *Chem. Soc. Rev.*, 2014, vol. 43, p. 5815.
8. Wu, Y., Yang, G.P., Zhao, Y., et al., *Dalton Trans.*, 2015, vol. 44, p. 3271.
9. Liu, B.B., Lin, X.L., Li, H., et al., *Cryst. Growth Des.*, 2015, vol. 15, p. 4355.
10. Lu, Z.Z., Zhang, R., Li, Y.Z., et al., *J. Am. Chem. Soc.*, 2011, vol. 133, p. 4172.
11. Wang, G.Y., Yang, L.L., Li, Y., et al., *Dalton Trans.*, 2013, vol. 42, p. 12865.
12. Ma, D.X., Li, B.Y., Zhou, X.J., et al., *Chem. Commun.*, 2013, vol. 49, p. 8964.
13. Xie, S.L., Wang, H.F., Liu, Z.H., et al., *RSC Adv.*, 2015, vol. 5, p. 7121.
14. Li, Y.-L., Wang, J., Shi, B.-B., et al., *Supramol. Chem.*, 2016, vol. 28, p. 640.
15. Rocha, J., Carlos, L.D., Paz, F.A.A., et al., *Chem. Soc. Rev.*, 2011, vol. 40, p. 926.
16. Wang, W.Y., Niu, X.L., Gao, Y.C., et al., *Cryst. Growth Des.*, 2010, vol. 10, p. 4050.
17. Wang, W.Y., Yang, Z.L., Wang, C.J., et al., *CrystEngComm*, 2011, vol. 13, p. 4895.
18. Shelddrick, G.M., *SHELXL-97, Program for the Solution and Refinement of Crystal Structures*, Göttingen: Univ. of Göttingen, 1997.
19. Guo, M.W., Chen, N., Gao, Y.C., et al., *J. Coord. Chem.*, 2012, vol. 65, p. 1724.
20. Shi, B.B., Zhong, Y.H., Guo, L.L., et al., *Dalton Trans.*, 2015, vol. 44, p. 4362.